arXiv:cond-mat/0306655v1 [cond-mat.soft] 25 Jun 2003

Monitoring Diffusion of Reptating Polymer Chains by Direct Energy Transfer Method: a Monte Carlo Simulation

Erkan Tüzel[†],[1,2] K. Batuhan Kısacıkoğlu,[1] and Önder Pekcan[1]

[1] *Department of Physics, Faculty of Sciences and Letters, Istanbul Technical University, Maslak 80626, Istanbul, Turkey*
[2] *Department of Physics, Faculty of Sciences and Letters, Işık University, Maslak, 80670, Istanbul, Turkey*

A kinetic Monte Carlo method was used to simulate the diffusion of reptating polymer chains across the interface. A time-resolved fluorescence technique conjunction with direct energy transfer method was used to measure the extend of diffusion of dye labeled reptating polymer chains. The diffusion of donor and acceptor labeled polymer chains between adjacent compartments was randomly generated. The fluorescence decay profiles of donor molecules were simulated at several diffusion steps to produce mixing of the polymer chains. Mixing ratios of donor and acceptor labeled polymer chains in compartments were measured at various stages (snapshots) of diffusion. It was observed that for a given molecular weight, the average interpenetration contour length was found to be proportional to the mixing ratio. Monte Carlo analysis showed that curvilinear diffusion coefficient is inversely proportional to the weight of polymer chains during diffusion.

I. INTRODUCTION

The diffusion of polymer chains across polymer-polymer interfaces has been of interest for more than a decade.[1, 2] One of the reason for the interest is that polymer diffusion across an interface is found to be important in technological processes, such as sintering of polymer powders, development of the strength of polymer powder by compression molding and annealing and the formation of latex films. Latex-film formation has been considered in the literature for over 50 years and is frequently used in the modern industry.[3, 4] The process of latex film formation has been divided into several stages. The generally accepted mechanisms consist of: (i) evaporation which brings the particles into some form of close packing; (ii) deformation of particles which leads to a structure without voids, although with the original particles still distinguishable; and (iii) diffusion of polymer chains across particle-particle boundaries, yielding a continuous film with mechanical integrity. Voyutskii proposed that physical contact between latex particles would not produce a mechanically strong continuous film if no external effect is applied.[5] In other words, in order to obtain a stable film it is necessary that the segments of polymer chains diffuse from one particle to another by forming a strong linkage between them. He described the process of diffusion with the word of "autohesion". For several decades, after Voyutskii's paper there have been only speculations about the process of diffusion during latex film formation. The developments in neutron scattering techniques have enabled the carrying out of experiments to study diffusion of polymer molecules across particle-particle boundaries. Important progress was made when small angle neutron scattering (SANS) technique was applied to study diffusion between particles of hydrogenated and deuterated acrylic latex particles.[6] Later, it was reported that increasing molecular weight and incompatibility lower the diffusion rate.[7] SANS was employed to measure the extend of diffusion in polystyrene (PS) latex having high molecular weight and small particle size, where an increase in the radius of gyration (R_g) of the polymer was observed when the system was heated above its T_g.[8]

The non-radiative direct energy transfer (DET) method conjunction with time resolved fluorescence (TRF) tecnique was first used to study polymer diffusion across particle-particle boundaries[9] to monitor concentration profiles of donor and acceptor dyes attached to polymers that are located initially in separate particles. As polymer diffusion occurs, mixing of donor (D) and acceptor (A) dyes can be measured by an increase in energy transfer between them. Early measurements using DET on poly (methyl methacrylate) (PMMA) latex particles prepared by nonaqueous dispersion polymerization found diffusion coefficients of the order of $10^{-15} cm^2 s^{-1}$ at temperatures between $400-450$ K. The film formation of a poly (butyl methacrylate) latex prepared via emulsion polymerization in water, was studied using the same technique. The diffusion coefficients ($10^{-16} cm^2 s^{-1}$) were determined using spherical diffusion model, and found to be dependent on both time and temperature. A decrease in diffusion rate with time was attributed to the effect of low molecular weight chains near the particle-particle surface dominating at early times. The DET method of data analysis was later developed for melt pressed PMMA particles.[10] It is observed that mass transfer increased with time to a power of 0.5 as in Fickian diffusion model for low molecular weight polymers. For high molecular weights, there is a distinct 0.25 power dependence that cannot be explained by a Fickian or reptation model.

Two reviews[1, 11] summarized experimental ap-

[†]Present address: University of Minnesota, School of Physics and Astronomy, 116 Church St. SE, Minneapolis, MN, 55455, USA

proaches and results in studying diffusion in latex systems up to the year of 1993 and 1994, respectively. Both papers reviewed the evidence of diffusion of polymers at particle-particle junction using transmission electron microscopy, SANS, atomic force microscopy and fluorescence techniques. Data analysis using DET and a fluorescence technique was later improved by taking into account the donor and acceptor concentration profiles during polymer diffusion, where a uniform acceptor concentration was considered around a donor in thin slices or shells.[12, 13] Further a model for DET was developed which considered the heterogeneity in the donor and acceptor concentration profiles,[14] where the diffusion coefficient of polymer chains obtained by different DET models. DET studies in latex blends, where one phase is far below its T_g and does not undergo any significant diffusion, found that the magnitude of energy transfer is proportional to the interfacial area. It was observed that organic solvents, which plasticize the latex, enhance the rates of polymer diffusion and the diffusion rate increased in the presence of cosurfactants.[15] At the times longer than the tube renewal time (escape time), the activation energy for diffusion was found 30 kcal/mol in the presence of cosurfactants, which is 48 kcal/mol in the neat polystyrene. Monte Carlo studies on diffusion of donor and acceptor dyes between the adjacent compartments were modeled by using Brownian motion.[16, 17, 18]

In this work Kinetic Monte Carlo (KMC) method was used to simulate the diffusion of polymer chains between the adjacent compartments of a cube where free energies and the potentials between molecules were not considered. These chains are labeled with either donor or acceptor dyes. Reptation of polymer chains were simulated using KMC method which produced more realistic diffusion results compared to previous studies.[16, 17, 18] The diffusion of donor and acceptor labeled polymer chains between adjacent compartments was randomly generated where each chain reptates according to de Gennes model.[19] The decay of the donor fluorescence intensity, $I(t)$ by DET was simulated at several diffusion steps and a gaussian noise was added to generate the time resolved fluorescence decay data. $I(t)$ decays were then fitted to the phenomenological equation

$$\frac{I(t)}{I(0)} = B_1 \exp(-t/\tau_0 - C(\frac{t}{\tau_0})^{1/2}) + B_2 \exp(-t/\tau_0) \quad (1)$$

where τ_0 is the fluorescence lifetime of donor and B_1 and B_2 are the pre-exponential factors. Here it is useful to define the mixing ratio K representing the order of mixing during diffusion of the donor and the acceptor labeled polymer chains as

$$K = \frac{B_1}{B_1 + B_2} \quad . \quad (2)$$

K was measured in terms of B_1 and B_2 for various molecular weights, M of polymer chains. Results were interpreted in terms of average interpenetration contour length, $\ell(t_r)$ and curvilinear diffusion coefficient, D_1.

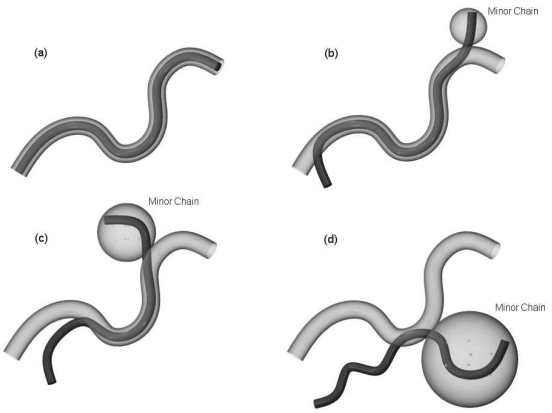

FIG. 1: A cartoon representation of a reptating polymer chain in a tube at different times (a,b,c and d). The memory of the initial tube is lost in Figure 1d. The picture also demonstrates the motion of minor chain during reptation.

II. THEORETICAL CONSIDERATIONS

A. Molecular Motion of Polymer Chains

The motion of individual chains in bulk polymeric materials or concentrated solutions of linear random-coil (Gaussian) chains has been modeled by the reptation theory of de Gennes[19] and Edwards.[20] In this model the polymer chain is confined to a tube which presents topological constraints to lateral motion of monomers imposed by the neighboring chains via entanglements. The motion of the chain is restricted to the curvilinear length of the tube, which is shown in Figure 1. As shown in Figure 1a, at time zero, the chain is in its initial tube which performs Brownian back and forth motion. Since the chain ends are free to move in any direction away from the tube, the memory of the initial tube position in space is gradually lost as shown in Figures 1b and 1c. Figure 1d presents the final stage of the reptation, i.e. just before the total escape of the chain from its original tube. At the time T_r, the escape time, the chain escapes or forgets its original configuration. As the chain is in a bulk polymeric system, it always creates a new tube after escaping from the previous one. The length of chain, $\ell(t_r)$ which escapes from the initial tube is also a random-coil chain which obeys Gaussian statistics and called the minor chain.[21, 22] During the process of reptation the length of the minor chain grows which is represented in Figure 1 by the growing spherical envelope. The mean square escape length of the minor chains, $< \ell^2 >$ is calculated by the following relation[21]

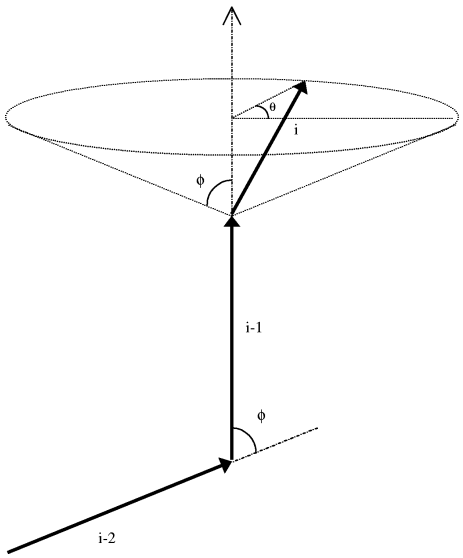

FIG. 2: Schematic picture of the bond and dihedral angles for the polymer chains. The bond angle ϕ is equal to 60^o, and the dihedral angles, namely θ, can be randomly chosen.

$$< \ell^2 >= 16\pi^{-1} D_1 t_r \quad . \tag{3}$$

where t_r is the diffusion time and D_1 is the curvilinear one-dimensional diffusion coefficient. The molecular weight dependence of D_1 and T_r are given by the following relations

$$D_1 \sim M^{-1} \tag{4}$$

and

$$T_r \sim M^3 \tag{5}$$

respectively.

The average interpenetration contour length, $\ell(t_r)$ of chain segments which have diffused across the interface is obtained from the minor chain model as[22]

$$\ell(t_r) \sim M^{-1/2} t_r^{1/2} \tag{6}$$

$$\ell_\infty \sim M \tag{7}$$

This property has the same scaling relation as the minor chain length, $< \ell >$.

B. Direct Energy Transfer Method

Time resolved fluorescence (TRF) in conjunction with DET method monitors the extent of diffusion of donor

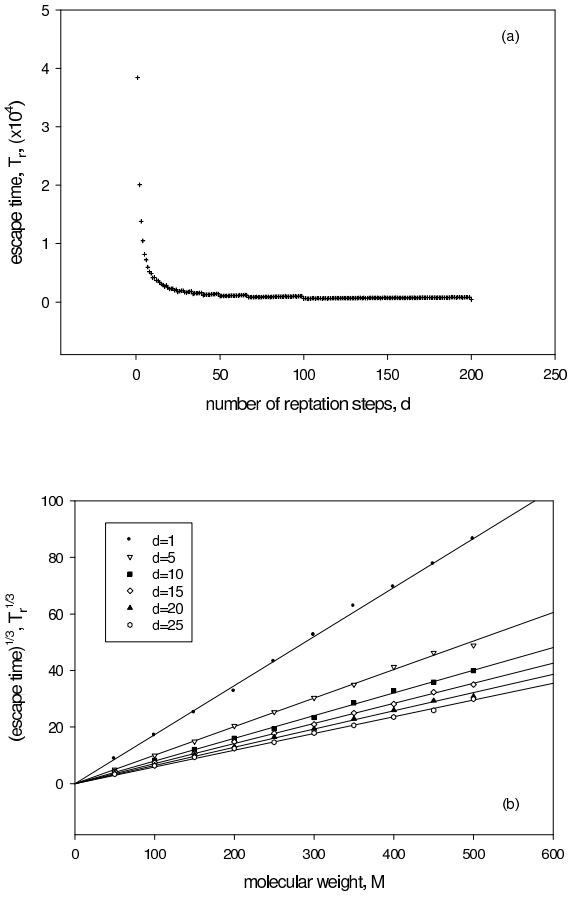

FIG. 3: The plot of a) escape time, T_r against the number of reptation steps, d, b) $(T_r)^{1/3}$ versus molecular weight, M, for different reptation steps, d, for a polymer chain containing 200 monomer units.

(D) and the acceptor (A) labeled polymer molecules. If the sample is made of a mixture of D and A labeled polymer chains where the diffusion takes place, after a period of time when the donor fluorescence profiles are measured, each decay trace provides a snapshot of the extent of diffusion.[9] This sample is considered to be composed of three regions; unmixed D, unmixed A and the mixed D - A region. The above model was first empirically introduced by the two component donor fluorescence decay.[23]

When donor dyes are excited using a very narrow pulse of light, the excited donor returns to the ground state either by emitting a fluorescence photon or through the nonradiative mechanism. For a well behaved system, after exposing the donors to a short pulse of light, the fluorescence intensity decays exponentially with time. However, if acceptors are present in the vicinity of the excited donor, then there is a possibility of DET from the excited donor to the ground state acceptors. In the classical

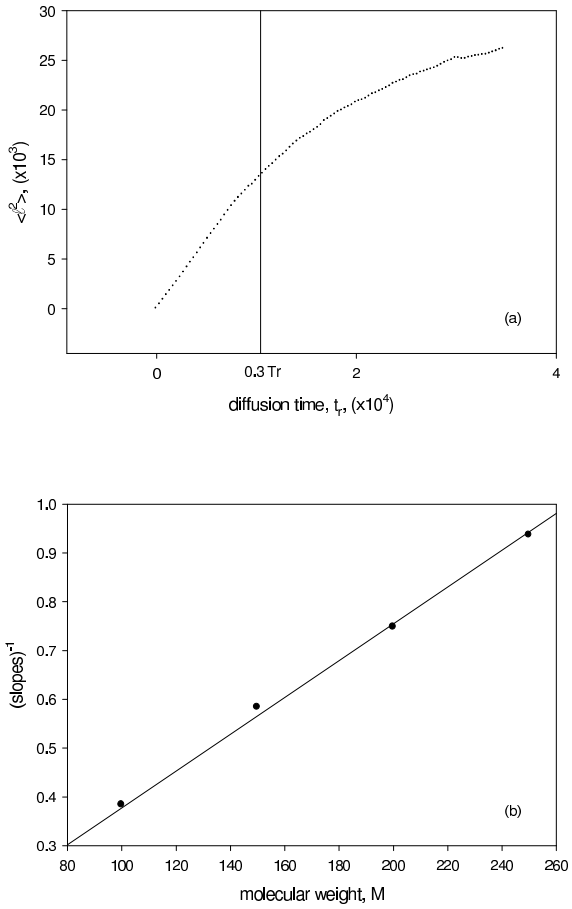

FIG. 4: The plot of a) mean square escape length, $< \ell^2 >$ of minor chain versus diffusion time, t_r, b) The inverse slope of $< \ell^2 >$ versus molecular weight, M. For a polymer chain of 200 monomer units.

problem of DET, neglecting back transfer, the probability of the decay of the donor at r_k due to the presence of an acceptor at r_i is given by[24]

$$P_k(t) = exp[-t/\tau_0 - w_{ik}t] \tag{8}$$

where w_{ik} is the rate of energy transfer given by Förster as

$$w_{ik} = \frac{3}{2}\kappa^2 \frac{1}{\tau_0}\left(\frac{R_0}{r_{ik}}\right)^6 \quad . \tag{9}$$

Here R_0 represents the critical Förster distance and κ is a dimensionless parameter related to the geometry of interacting dipole. If the system contains N_D donors and N_A acceptors, then the donor fluorescence intensity decay can be derived from the equation (9) and given by[10, 11]

$$\frac{I(t)}{I(0)} = \exp(-t/\tau_0)\frac{1}{N_D}\int n_D(r_k)dr_k \times \prod_{i=1}^{N_A}\frac{1}{N_A}\int n_A(r_i)dr_i \exp\left(-w_{ik}t\right) \quad . \tag{10}$$

Here n_D and n_A represent the distribution functions of donors and acceptors. In the thermodynamic limit equation (10) becomes

$$\frac{I(t)}{I(0)} = \exp(-t/\tau_0)\frac{1}{N_D}\int n_D(r_k)dr_k \times \exp(-\int n_A(r_i)dr_i(1-\exp\left(-w_{ik}t\right))) \quad . \tag{11}$$

This equation can be used to generate donor decay profiles by Monte-Carlo techniques. It is shown that the equation (11) reduces to a more simple form which can be compared to the experimental data.[25] The simplification is summarized below for clarity. Changing to the coordinate $r_{ik} = r_i - r_k$ leads to,

$$\frac{I(t)}{I(0)} = \exp(-t/\tau_0)\frac{1}{N_D}\int n_D(r_k)dr_k \times \prod_{i=1}^{N_A}\int_{r_K}^{R_g - r_K} n_A(r_{ik}+r_k)dr_{ik}\exp\left(-w_{ik}t\right) \tag{12}$$

where R_g is an arbitrary upper limit. Placing a particular donor at the origin and assuming that the mixed and unmixed regions are created during diffusion of D and A, equation (12) becomes

$$\frac{I(t)}{I(0)} = B_1\exp(-t/\tau_0)\prod_{i=1}^{N_A}\frac{1}{N_A}\int_0^{R_g} n_A(r_{ik})dr_{ik} \times \exp\left(-w_{ik}t\right) + B_2\exp(-t/\tau_0) \tag{13}$$

where

$$B_{1,2} = \frac{1}{N_D}\int_{1,2} n_D(r_k)dr(k) \tag{14}$$

represent the fraction of donors in mixed and unmixed regions respectively. The integral in equation (13) produces a Förster type of function[26, 27]

$$\prod_{i=1}^{N_A}\frac{1}{N_A}\int_0^{R_g} n_A(r_{ik})dr_{ik}exp(-w_{ik}t) = exp(-C(\frac{t}{\tau_0})^{1/2}) \tag{15}$$

where C is proportional to acceptor concentration. Eventually, one gets equation (1) for the fluorescence intensity.

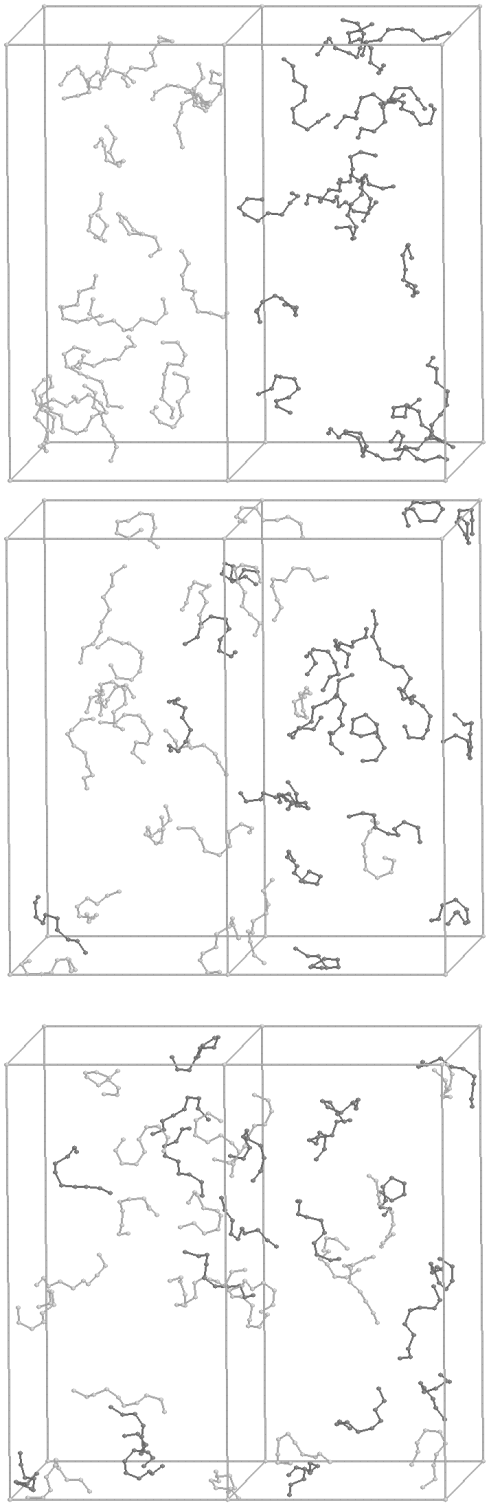

FIG. 5: Snapshots of diffusion between adjacent compartments of the cube with the size $L \times L \times L (L = 30)$. Donor, D labeled chains in the right compartment are presented in black for clarity. The chains consist of 10 units and the number of chains in each compartment is taken to be 20. The grey colored chains represent the ones that are labeled by acceptors, A.

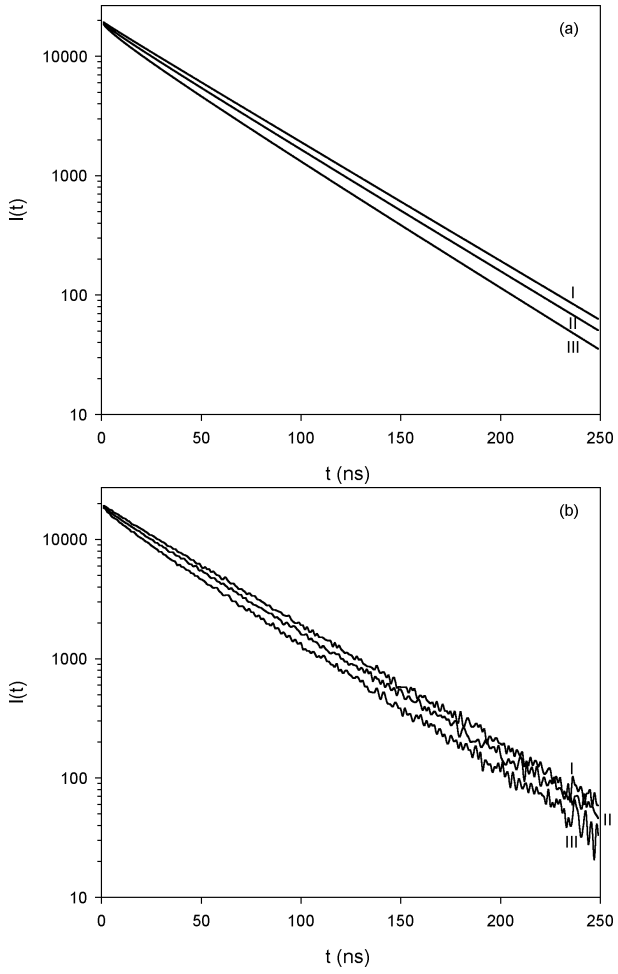

FIG. 6: a) Donor decay profiles at several diffusion steps for $M = 100$ and $d = 10$. Where the mixing ratios are taken as I) $K = 0.1$, II) $K = 0.5$, III) $K = 0.9$, b) Noisy decay profiles for the above picture.

III. RESULTS AND DISCUSSION

A. Freely Rotated Chain Model for Reptation

The polymer chains were constructed from the rod like segments which were connected to each other with a bond angle, $\phi = 60^o$. The dihedral angle, θ was chosen randomly as seen in Figure 2. The length of a segment was taken to be unity and the molecular weight, M of the chain was assumed to be proportional to the number of rods (monomers) that chain contains. Monte Carlo simulations were performed so that the chains move according to the reptation model, where for each reptation step, while a segment from the tail disappears, another segment is added to head or vice versa. In other words the chain is being trapped in a hypothetical tube, leaves the tube in a randomly chosen directions, creating a segment of minor chain as shown in Figure 1. A unit of diffu-

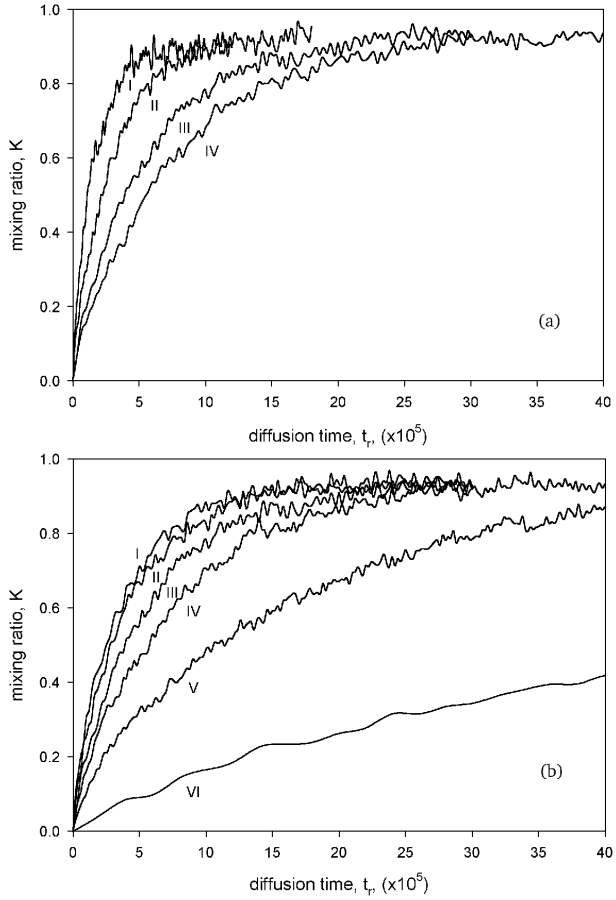

FIG. 7: a) Variation of K with respect to diffusion time, t_r for different molecular weights, I) $M = 100$, II) $M = 150$, III) $M = 200$, IV) $M = 250$ for $d = 15$, b) The plots K versus diffusion time, t_r for different d values; I) $d = 25$, II) $d = 20$, III) $d = 15$, IV) $d = 10$, V) $d = 5$ and VI) $d = 1$, for $M = 200$.

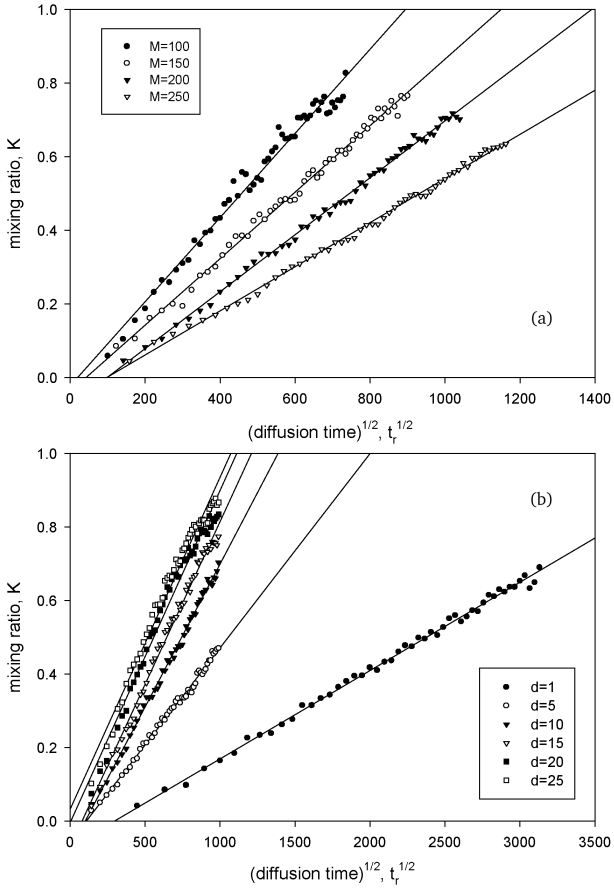

FIG. 8: a) K versus ${t_r}^{1/2}$ plots for different values of M, b) K versus ${t_r}^{1/2}$ plots for different values of d. Slopes of linear fits produce a in equation (17).

sion time, t_r was defined for a single reptation step of a chain that has 100 monomers. For instance single reptation step of a chain with 200 monomers takes 2 units of t_r. The number of reptation steps in chosen direction for each simulation was defined as d which controls the escape time i.e. an increase in d shortens the escape time, T_r. Figure 3a presents the behavior of escape time, T_r against d for a polymer chain which has 200 monomer units. Here T_r was determined with a separate program which uses the same reptation algorithm as in the simulation programs. In this program a single chain reptates until it escapes from its initial tube and then T_r is recorded. The average T_r is calculated from several runs. It is seen in Figure 3a that as d is increased T_r decreases i.e. chain escapes quicker from its initial tube. The relation between T_r and molecular weight, M for different d values are shown in Figure 3b, where linear behavior of $T_r^{1/3}$ versus M suggest that polymer chains reptate in accordance with equation (5) in our KMC simulations. The steepest curve for $d = 1$ predicts that corresponding polymer chain needs longer time than others to escape from its tube. However when chain reptates with $d = 25$ escape time, T_r is very short for all molecular weights.

The minor chain growth was monitored by observing the mean square escape length $< \ell^2 >$ versus diffusion time, t_r where $< \ell^2 >$ was determined using the same separate program which determines T_r. This program reptates a single chain and records the minor chain length. The average was calculated after several runs of this program. Results are shown in Figure 4a for a chain contains 200 monomer units, where it is seen that the region between $t_r = 0$ to $t_r = 0.3T_r$ presents linear relation which accords with equation (3). The slope of the curves in the linear region is proportional to the curvilinear one dimensional diffusion coefficient, D_1 which were produced for various molecular weights, M. The inverse of the slopes, $(slope)^{-1}$ are plotted versus M in Figure 4b where the perfect linear relation is in accord with equation (4) i.e. $D_1 \sim M^{-1}$.

B. Energy Transfer for Chain Diffusion

Diffusion of D and A labeled chains between adjacent compartments was simulated using above KMC algorithm. The sample cube with the side, $L = 500$ units, was divided into two equal compartments which contain donor, D and acceptor, A labeled chains respectively, presented in Figure 5. Each compartment contains 500 chains and one percent of monomers in each chain labeled with donors or acceptors. Here one has to be noticed that chains are chosen quite short and the system is very dilute for the reptation model. In fact, here the reptation algorithm is designed so that it operates as if the chains are in the melt system. This algorithm is chosen to avoid the immediate decay of donors where the chains are kept far away from each other and still perform the reptation motion. One may attemp to solve this problem by filling up the system with unlabeled chains by designing more realistic algorithm, which, however then spends tremendous computer time to perform reptation motion for all chains. Since these unlabeled chains have no contribution to the DET, using the reptation algorithm in the dilute system saves considerable amount of computer time and still mimics the realistic reptation motion. The measured reptation parameters have shown that the chosen dilute system and the reptation algorithm work quite well and the attempt to study the DET during diffusion is reliable.

The decay of donor intensity by DET was simulated for the possible configurations at the end of each 10^4 steps of diffusion, therefore the snapshots of diffusion processes can be monitored quite clearly and accurately. Reflected boundary conditions were used from the sides of the cube. For the configurations of $d = 1$ the decay of donor intensity was simulated after $0.5 \times 10^5 - 10^5$ steps of diffusion because diffusion process for this case takes much longer time. Snapshots of the diffusing polymer chains between adjacent compartments in a cube are shown in Figures 5a, b and c at various diffusion steps. The D and A labeled chains are colored in black and grey, respectively, for clarity.

The donor decay profiles were generated using equation (11). The w_{ik} values for each donor-acceptor pair were obtained from equation (9) using a Förster distance of 26 units. The parameter κ^2 was chosen as 0.476, a value appropriate for immobile dyes,[17] and the donor lifetime τ_0 was taken as 44ns. Then equation (11) was used to simulate the donor intensity $I(t)$ i.e. fluorescence decay profile. $I(0) = 2 \times 10^4$ was chosen and the decay profiles were obtained for a 250ns interval, divided into 250 channels of 1ns each. The fluorescence decay profiles $I(t)$, for the polymer chains with $M = 100$ and $d = 10$ are given in Figure 6a at various diffusion steps, i.e. various mixing ratios, K. In order to obtain more realistic decay profiles, gaussian noise was added to the original decay profiles using Box, Muller and Marsaglia (1958) algorithm.[28] Here, one may also take into account the effect of the lamp profile when calculating the decay profiles.[17, 18] To do so the decay profiles generated by the Monte Carlo simulation should be convolved with experimental lamp profile, then the experimentally measured $\psi(t)$ is obtained by convolution of $I(t)$ with the instrument response function $L(t)$, as

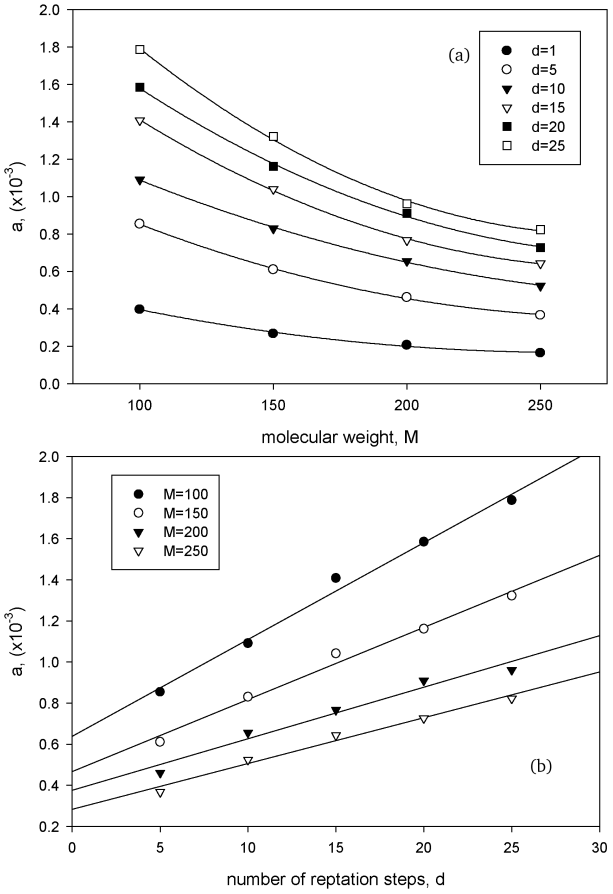

FIG. 9: a) The dependence of a on molecular weights, M, for various values of d, b) Plots of the variation of a with d, for different values of M. The linear relation between a and d are shown by the regression lines.

$$\psi(t) = \int_0^t L(t)I(t-s)ds \ . \qquad (16)$$

In this work generated decay profiles were used, namely $I(t)$.[16] This assumption is valid if one uses a delta, δ function light source (e.g. a very fast laser) as the lamp profile. In this case no convolution is needed and equation (16) produces $I(t)$. The noisy decay profiles of donors for a δ function light source are presented in Figure 6b at various diffusion steps, similar to Figure 6a.

C. Extend of Diffusion

In order to calculate the mixing ratio, K defined in equation (2), the decay profiles were fitted to equation (1)

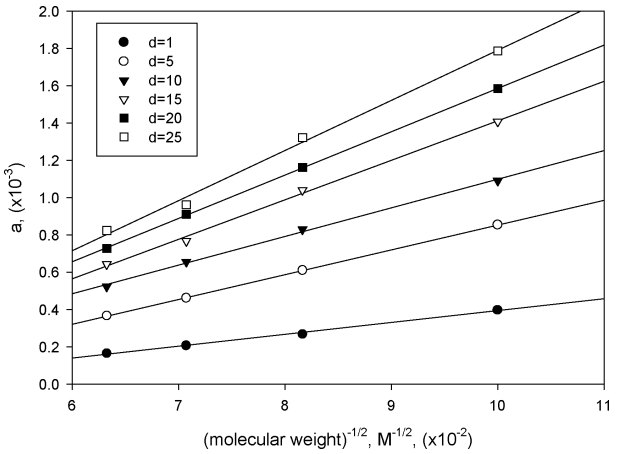

FIG. 10: a versus $M^{-1/2}$ plots for different values of d. The linear regression lines show the goodness of fit to equation (18).

using Levenberg-Marquart[29] algorithm. During curve fitting process $C(=1)$ and $\tau_0(=44)$ were kept constant and B_1 and B_2 values were varied. Since C and τ_0 were fixed, the fitting procedure directly produced B_1 and B_2 values, which are a pre-exponential factor in mixed and unmixed regions. At early times of diffusion B_2 dominates by presenting low mixing, however at later times B_1 increases and dominates the mixing ratio. Here basically simulation of decay curves are essential in calculation of B_1 and B_2 values. More than 10^4 decay profiles were fitted and the goodness of fitting was accepted as $\chi^2 < 1.5$. The B_1 and B_2 values were used to obtain K values at diffusion steps during reptation of polymer chains. Figure 7a presents the variation of K with respect to the diffusion time, t_r for chains at different molecular weights, $M(100, 150, 200, 250)$ for $d = 15$. As seen in Figure 7a mixing of diffusing chains are much faster for the low molecular weight samples (I,II) than high molecular weight samples (III,IV). When the molecular weight is increased diffusion slows down as expected. Diffusion for different d values is also shown in Figure 7b, K versus diffusion time are plotted for various d values $(1, 5, 10, 15, 20, 25)$ for chains at $M = 200$, where it is seen that increase in d cause increase in mixing of diffusing chains. In order to quantify the above results the following equation was employed

$$K = at_r^{1/2} \ . \tag{17}$$

Here we intent to elaborate the equation (6), where the molecular weight, M can be related with a in equation (17). The fits of the data in Figures 7a and 7b to equation (17) are given in Figures 8a and 8b, respectively. The slopes of the linear relations in Figure 8 produce "a" values which are plotted versus M and d in Figures 9a and 9b, respectively. Curves in Figure 9a predict that as M is increased, a decreases. In order to determine the behavior of a with respect to M; an a versus $M^{-1/2}$ plot is presented in Figure 10 where the following relation is obeyed.

$$a \sim M^{-1/2} \tag{18}$$

Here one may speculate that mixing ratio, K is most probably proportional to the average interpenetration contour length, $\ell(t_r)$ according to equation (6). In other words K is the measure of $\ell(t_r)$ which is quite important in determining the mechanical properties of polymeric materials.[22]

On the other hand the plot in Figure 9b suggests that as d is increased, a increases which predicts that as the chains reptate faster, the mixing ratio, K increases as expected. It is evident that since small chains reptate faster, they can mix much quicker than high molecular weight chains. Here one may also argue that the root square of equation (3) suggests that $D_1 \sim M^{-1}$ relation holds for our simulation results.

IV. CONCLUSION

In conclusion this paper has presented a Kinetic Monte Carlo method which can be used to simulate the interdiffusion of reptating polymer chains across the interface. It was shown that Equation (1) can be succesfully applied to measure the extend of interdiffusion of reptating donor and acceptor labeled polymer chains. Monte Carlo results have shown that the curvilinear diffusion coefficient is inversely proportional to the weight of the polymer chains and for a given molecular weight the average interpenetration contour length was found to be proportional to the extent of interdiffusion.

[1] Ö. Pekcan, *Trends in Polymer Sci.* **1997**, 5, 177.
[2] H. H. Pham , J. P. S. Farinha and M. A. Winnik, *Macromolecules*, **2000**, 33, 5850.
[3] S. Mazur, *"Polymer Powder Processing"*, N. Rosenweig, Eds., John Wiley and Sons, New York 1996.
[4] J. L. Keddie, *Material Sci. and Eng.* **1997**, 21, 101.
[5] S. S. Voyutskii, *"Autohesion and adhesion of high polymers"*, Interscience Publisher, New York 1963.
[6] K. Hahn, G. Ley, H. Schuller, R. Oberthum, *Colloid Polym. Sci.* **1986**, 264, 1092.

[7] K. Hahn, G. Ley, R. Oberthum, *Colloid Polym. Sci.* **1988**, 266, 631.

[8] K. D. Kim, L. H. Sperling, A. Klein, *Macromolecules* **1993**, 26, 4624.

[9] Ö. Pekcan, M. A. Winnik and M. D. Croucher, *Macromolecules* **1990**, 23, 2673.

[10] Y. Wang and M. A. Winnik, *Macromolecules* **1993**, 26, 3147.

[11] Y. Wang and M. A. Winnik, *J. Phys. Chem.* **1993**, 97, 2507.

[12] J. P. S. Farinha, J. M. G. Martinko, A. Yekta, M. A. Winnik, *Macromolecules* **1995**, 28, 6084.

[13] G. A. O' Neil, J. M. Torkelson, *Macromolecules* **1997**, 90, 5580.

[14] J. P. S. Farinha, J. M. G. Martinko, A. Yekta, M. A. Winnik, *J. Phys. Chem.* **1996**, 100, 12552.

[15] A. Juhue, J. Lang, *Macromolecules* **1994**, 27, 695.

[16] E. Tüzel, K. B. Kısacıkoğlu and Ö. Pekcan, *Polymer* **2000**, 41, 7539.

[17] K. S. Güntürk, A. T. Giz and Ö. Pekcan, *Polymer* **1998**, 39, 10.

[18] K. S. Güntürk, A. T. Giz and Ö. Pekcan, *Eur. Polym. J.* **1998**, 34, 789.

[19] P. G. de Gennes, *"Scaling Concepts in Polymer Physics"*, Cornell University Press 1988.

[20] S. F. Edwards, *"Molecular Fluids"*, R. Balian and G. Weill, Eds., Gordon and Breach, New York 1976.

[21] Y. H. Kim, R. P. Wool, *Macromolecules* **1983**, 16, 1115.

[22] R. P. Wool, B. L. Yuan, O. J. Megarel, *Polymer Eng. Sci.* **1989**, 29, 1340.

[23] M. A. Winnik, Ö. Pekcan, M. D. Croucher, *"Scientific Methods for the Study of Polymer Colloids and their Applications"*, F. Condon, R. H. Ottewill, Eds., NATO ASI, Kluver Acad. Pub. 1988.

[24] T. H. Förster, *Ann. Phys.* **1948**, 2, 55.

[25] P. R. Sperry, B. S. Snyder, M. L. O' Downd and P. M. Lesko, *Langmuir* **1994**, 10, 2619.

[26] J. Klafter and A. Blumen, *J. Chem. Phys.* **1984**, 80, 875.

[27] J. Bauman and M. D. Fayer, *J. Chem. Phys.* **1986**, 85, 408.

[28] W. H. Press, S. A. Teukolsky, W. T. Vetterling, B. P. Flannery, *"Numerical Recipes In C"*, 2nd edition, Cambridge University Press 1992.

[29] P. R. Bevington, D. K. Robinson, *"Data Reduction and Error Analysis for the Physical Sciences"*, 2nd edition, McGraw-Hill Inc. 1992.